Catal Lett (2008) 124:111–117
DOI 10.1007/s10562-008-9433-5

Designed Highly Effective Photocatalyst of Anatase TiO_2 Codoped with Nitrogen and Vanadium Under Visible-light Irradiation Using First-principles

Zongyan Zhao · Qingju Liu

Received: 19 December 2007 / Accepted: 7 February 2008 / Published online: 26 February 2008

Abstract The supercells of pure anatase TiO_2, nitrogen and/or vanadium doping anatase TiO_2 were calculated by first-principles with the plane-wave ultrasoft pesudopotentials method. The effects of different ions doping on the crystal structure, electronic structure, optical properties and photocatalytic activity were investigated by means of the calculational data. At the same time realizing visible-light response, nitrogen and vanadium codoping TiO_2 photocatalysts have strong redox potential, and its photocatalytic efficiency would be remarkably improved due to enhancement of electron–hole pairs' separation. The conclusions would have important significance for understanding and further developing of TiO_2 photocatalyst that are activity under visible-light irradiation.

Keywords Anatase TiO_2 · Codoping · Photocatalyst · First-principle calculation

1 Introduction

Energy depleting and ecological environment deteriorating are two important issues which urgently need to be solved in today's society. In many means of settlement, heterogeneous photocatalysis based on oxide semiconductor is a promising technology, and has become one of the most active research fields in recent years. So far, researchers developed many materials that have the potential of application to act as photocatalysts, including TiO_2, $SrTiO_3$, α-Fe_2O_3, WO_3, ZnO, Bi_2WO_6 and ZnS. Among them, TiO_2 has been attracted extensively attention as an ideal photocatalytic material because of its excellent properties, such as nontoxic, highly oxidative, chemically stable and inexpensive [1–3]. However, as a wide band gap oxide semiconductor ($E_g = 3.23$ eV), anatase TiO_2 only shows photocatalytic activity under UV-light irradiation ($\lambda < 384$ nm) that accounts for only a small fraction ($\sim 5\%$) of the solar energy. The sun can provide an abundant source of photons, and the visible-light ($\lambda = 400$–700 nm) accounts for a large fraction ($\sim 45\%$), so its solar energy utilization is very low [4]. Furthermore, its photo quantum yield value is also very low due to its photoexcited electron–hole pairs easily recombining. Therefore, to develop highly effective TiO_2 photocatalyst, which has high photo quantum yield value and strong redox potential with suitable band structure responsive to visible-light irradiation, is the most challenging subject in present photocatalytic research.

Recently, many attempts have been made to improve the photocatalytic performance of TiO_2 under visible-light irradiation, such as transition metal [5] or nonmetal [6, 7] doping, noble metal loading [8], semiconductor compounding [9], organic dye sensitizing [10]. In these methods, ion doping is considered as one of the most efficient methods. According to the semiconductor theory, introducing defect (impurity atom, vacancy, etc.) into TiO_2 can cause certain distortion for local lattice potential. This distortion equals to introduce perturbation for the lattice potential; it will be having some corresponding impurity energy levels in the band structure. These impurity energy levels (donor or acceptor) will act as the capture trap for its photoexcited carriers that are produced by intrinsic excitation. The deep potential capture trap often becomes

Z. Zhao · Q. Liu (✉)
Yunnan Key Laboratory Nanomaterials & Nanotechnology, Yunnan University, Kunming, Yunnan 650091, People's Republic of China
e-mail: qjliu@ynu.edu.cn

recombination center; but the appropriate amount of shallow potential capture trap can promote the photoexcited carriers' internal diffusion process, which can greatly extend their lifetime and reduce their recombination rate, resulting in enhancement of the photocatalytic activity of TiO_2 [11]. However, ion-doping also could change the band structure of TiO_2—some dopants might narrow its band gap, and the redox ability of TiO_2 is related with its band edge position. Moreover semiconductor's band gap is smaller; the recombination rate of photoexcited carriers is greater. Therefore band gap narrowing can cause the redox ability of TiO_2 to be weakening and the recombination rate of photoexcited carriers to be greatening. This is an extremely contradictory problem at present. So Asahi et al. [6] have set some requirements for ion-doping: (1) doping should produce states in the band gap of TiO_2 that absorb visible light; (2) the conduction band minimum (CBM), including subsequent impurity states, should be as high as that of TiO_2 or higher that the H_2/H_2O level to ensure its photoreduction activity; and (3) the states in the gap should overlap sufficiently with the band states of TiO_2 to transfer photoexcited carriers to reactive sites at the catalyst surface within their lifetime.

The previous research mostly have been concentrated on the single ion-doping into TiO_2, but a few latest research show that different ions codoping into TiO_2 can further to enhance its optical absorption scope and photocatalytic activity [12–14]. Although, different ions codoping into TiO_2 has been a hot topic of experimental study, it remains difficult to make direct comparisons and unifying conclusions due to the widely varying experimental conditions, sample preparation and the determination of photoreactivity, and most research are only focus on their application performance. At the same time, because of lack of the detailed microscopic information about effects of ion doping on crystal structure and electronic structure, there is still much dispute about these issues. Comparing with experimental investigation, the theoretical analysis by computer simulation is expected to clarify the ion-doping effects in detail, because it can overcome the effects of complex experimental factors. Thus, it is very favorable to in-deep analyze the modification mechanism of ion doping and to design more reasonable and practicable highly effective TiO_2 photocatalyst. For this purpose, in this article, the plane-wave ultrasoft psedopotential (PW-USP) method within the framework of the first-principles has been used to design a highly effective photocatalyst of anatase TiO_2 codoped with nitrogen and vanadium. So, we calculated the electronic structure and optical properties of N + V-doped anatase TiO_2, and compared them with that of N-doped, V-doped and pure anatase TiO_2, in order to clarify how these ions impact the photocatalytic activity of TiO_2.

2 Calculation Models and Methods

Anatase TiO_2 has a tetragonal structure (space group: $I4_1/amd$, local symmetry: D_{4h}^{19}) and contains two titanium atoms and four oxygen atoms in the unit cell. Our models ($2 \times 2 \times 1$ supercell) consisted of eight unit cells stacked along the a-axes and b-axes, as shown in Fig. 1. In N + V-doped TiO_2 model, a Ti atom was substituted by a vanadium atom or an O atom was substituted by a nitrogen atom. Thus, one supercell consisted of 15 titanium atoms, 31 oxygen atoms, one vanadium atom and one nitrogen atom. The atomic concentration of impurity was about 2.08% (atomic fraction) in total, which was comparable to that used in the experiments. The other models are created by the same method.

All calculations were performed with the CASTEP module in Materials Studio 3.2 developed by Accelrys Software Inc. [15]. The wave functions of the valence electrons were expanded using a plane wave basis set within a specified energy cutoff that was chosen as 380 eV. The electronic exchange-correlation energy was treated within the framework of the local density approximation (LDA: CA-PZ) [16, 17]. The ultrasoft pseudopotential was chosen in the calculation, and its representation was in the reciprocal space, because it has several advantages both in efficiency and veracity. The Monkhorst–Pack scheme K-points grid sampling was set as $3 \times 7 \times 3$ for the irreducible Brillouim zone. A $45 \times 24 \times 54$ mesh was used for fast Fourier transformation. The convergences were set as 5×10^{-4} nm for maximum displacement tolerances, 0.1 eV/nm for maximum force, 0.02 GPa for maximum stress and 5×10^{-6} eV/atom for total energy change in the geometry optimization.

In order to get accurate results that can be compared with experimental results, we firstly optimized the crystal structures and atomic coordinates, which obtained by minimizing the total energy and atomic forces. In our

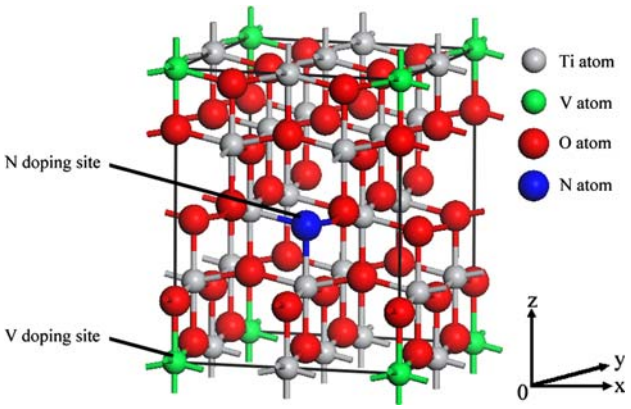

Fig. 1 Supercell model for N + V-doped anatase TiO_2 in the present work and the site of dopants

calculations, the cell parameters had optimized during the geometry optimization, in addition to the atomic coordinations. This is done by performing an iterative process in which the coordinates of the atoms and the cell parameters are adjusted so that the total energy of the structure is minimized. By doing so, we could obtain stable structures for all the models. Then we calculated electronic structures and optical properties of the optimized supercells. In optical properties calculations, we used unpolarized polycrystalline models and "scissors operators" [18] which were introduced to shift all the conduction levels to meet with the measured value of the band gap.

3 Results and Discussions

By optimizing the pure anatase TiO_2 supercell, we got the lattice parameters as follows: $a = b = 3.7436$ Å, $c = 9.4779$ Å, $d_{ap} = 1.9695$ Å, $d_{eq} = 1.9138$ Å, $2\theta = 155.917°$. They were in good agreement with experimental results [19]: $a = b = 3.7848$ Å, $c = 9.5124$ Å, $d_{ap} = 1.9799$ Å, $d_{eq} = 1.9338$ Å, $2\theta = 156.230°$. This result implies that our calculation methods are reasonable, and the calculated results should be authentic.

We analyzed the relative difficulty for different ions doping into anatase TiO_2 by impurity formation energies that is a widely accepted method. When the TiO_2 crystal react with nitrogen and/or vanadium, a few lattice oxygen atoms are replaced by nitrogen atom, and/or a few titanium atoms are replaced by vanadium atoms. Finally, the nitrogen and/or vanadium doping TiO_2 is obtained along with oxygen emission and/or titanium metal formation. According to the law of energy conservation, before and after the reaction, the difference between the energy of total systems is the energy that is required for the products. Namely, it is the impurity formation energy. In present work, the impurity formation energy (E_f) is defined as the following formula [20]:

$$E_f = E_{TiO_2:D} - E_{TiO_2} - \frac{1}{2}E_{N_2} - E_v + \frac{1}{2}E_{O_2} + E_{Ti} \quad (1)$$

where $E_{TiO_2:D}$, and E_{TiO_2} are the total energy of N + V-doped TiO_2, pure TiO_2 in the same size supercells. E_{N_2} and E_{O_2} are the energy of N_2 and O_2 gas molecular, E_v and E_{Ti} are the energy of bulk V and Ti metal, respectively. The calculated results were shown in Table 1. The results agree nicely with experimental observation and other theoretical method calculations [21, 22]. According to the results, we discover that the E_f of N + V-doped is larger than others. As a consequence, the synthesis of the N + V-doped TiO_2 becomes relatively difficult in the experiment because much larger formation energy is required.

Sato et al. [23] reported that the local internal fields due to the dipole moment of distorted octahedral can promote the charges separation in the initial process of photoexcitation, and are useful for enhancing photocatalytic activity. In Table 1, the lattice distortions, average bond lengths, average net charge by Mulliken population analysis and average dipole moments of octahedral in different ions doped anatase TiO_2 by geometry optimizing were given. The changes of cell volume, bond length and charge on atoms result in that the center of the gravity of negative electric charges would be deviated from the position of Ti^{4+} ion in TiO_6 octahedron and its dipole moment would not be still zero. The average dipole moments of TiO_6, TiO_5N and VO_6 that are averaged the magnitude of dipole moment neglecting the direction are obviously increased. Increasing of the internal fields, the separation of photoexcited electron–hole pairs would be easier. So that nitrogen doping or vanadium doping can greatly enhance the photocatalytic activity of TiO_2. This conclusion is consistent with the experimental results in recent literatures [24, 25]. For N + V-doped TiO_2, these changes are more obvious than that of N-doped or V-doped TiO_2. This means that nitrogen and vanadium codoping can further enhance the photocatalytic activity of TiO_2 comparing with single ion doping.

In order to conveniently compare the electronic structures of different ions doping models, we set the same K-points mesh to sample the first Brillouim zone for all models. The calculated band gap of pure anatase TiO_2 was 2.55 eV, as shown in Fig. 2, which is similar to the reported results [26, 27], but underestimated comparing with the experimental $E_g = 3.23$ eV [28] due to the limitation of DFT: the discontinuity in the exchange-correlation potential is not taken into account within the framework of DFT [29, 30]. The calculated band structures of N-doped, V-doped and N + V-doped are displayed in Fig. 2, respectively. In these figures, we can see that the energy levels are split because of decrease of their degree of degeneracy and crystal symmetry. If regardless the impurity energy levels, the band gaps are broadened to 2.57, 2.78, and 2.61 eV, respectively. For N-doped, three isolated impurity energy levels are located just above the top of the VB of TiO_2. For V-doped TiO_2, three isolated impurity energy levels are located just below the bottom of the CB of TiO_2. These impurity energy levels sufficiently overlap with valence band maximum (VBM) or CBM of TiO_2. For N + V-doped TiO_2, the splitting of energy levels become obvious. And the overlapping between impurity energy levels and VBM or CBM is more obviously than that of single ion doping, so we only found two isolated energy states above the top of VB. Thus nitrogen and vanadium codoping can further improve the transfer of photoexcited carriers to reactive sites.

Table 1 Formation energies, lattice distortions, average bond lengths, average net charges and average dipole moments of different ions doped TiO_2 by geometry optimizing

	E_f (eV)	Bond length (Å)			ΔV (Å^3)	Net charge (e)				Dipole moment (Debye)		
		Ti–O	N–O	V–O		Ti	O	N	V	TiO_6	TiO_5N	VO_6
Pure TiO_2		1.9363				1.270	−0.630			0.0000		
N-doped	5.422	1.9347	1.9642		1.029	1.258	−0.631	−0.560		0.0300	1.7099	
V-doped	2.714	1.9329		1.8870	−2.664	1.264	−0.625		1.120	0.0281		0.0000
N + V-doped	6.489	1.9403	1.8751	1.8703	−1.346	1.255	−0.621	−0.660	1.120	0.1674	2.1980	0.7091

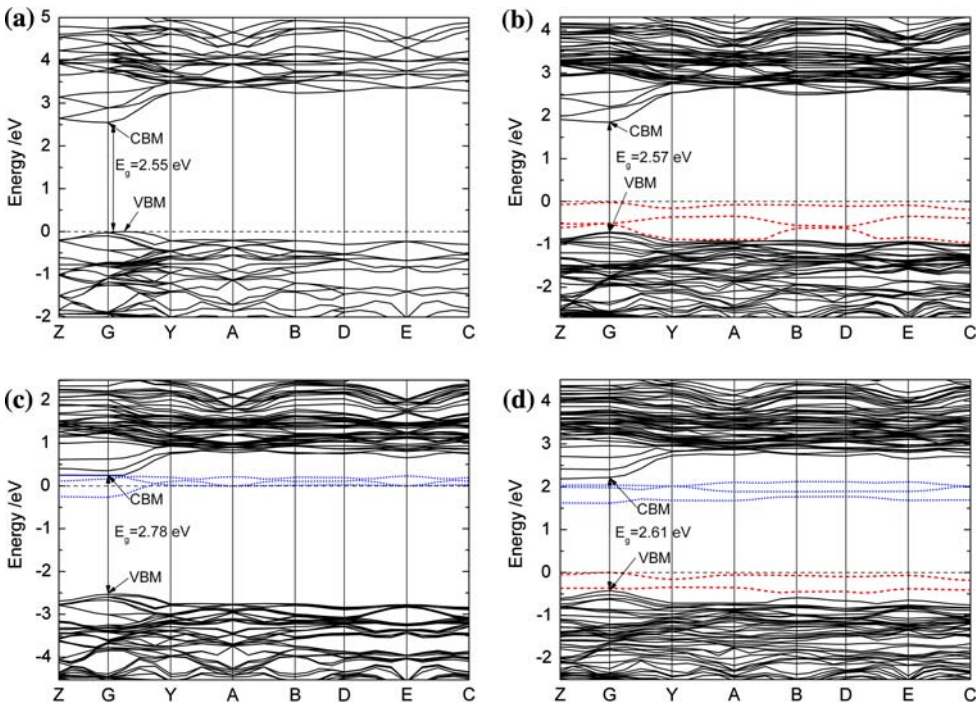

Fig. 2 Calcualted band structure of (**a**) pure TiO_2, (**b**) N-doped TiO_2, (**c**) V-doped TiO_2, and (**d**) N + V-doped TiO_2 along the symmetry lines of the first Brillouin zone

To further understand the origin of the band gap changes, the calculated total density of states (TDOS) and partial density of states (PDOS) (as depicted in Fig. 3) are inspected. In the pure TiO_2, VB and CB consist of both the O 2p states and Ti 3d states. Because the Ti 3d states is split into two parts (the t_{2g} and e_g states) in an octahedral ligand field with O_h symmetry, the CB is divided into the lower and upper parts. In summary, the calculated electronic structures described in this work are consistent with the results from other theoretical methods [31]. It is clear from these plots that the N 2p states or V 3d states are somewhat delocalized, thus greatly contributing to the formation of impurity energy levels by hybridized with O 2p states, Ti 3d states. The hybrid effect is very in favor of the migration of photoexcited carriers and the process of photocatalysis [2, 32]. Because of these impurity energy levels in the band gap, the electrons in the VB can be excited to them and then subsequently excited to the CB by absorption of visible-light. So these impurity energy levels are beneficial for extending the sensitive light wavelength towards visible-light region. Owing to the shallow acceptor (for N-doped TiO_2) or shallow donor (for V-doped TiO_2) would be act as capture trap for photoexcited holes or electrons, the impurity energy levels at VBM or CBM could reduce the recombination rate of photoexcited carriers. Thus they are very crucial for the enhancement of the photocatalysis efficiency. Furthermore, for N + V-doped TiO_2, it simultaneously process shallow acceptor and shallow donor, and the distance between acceptor and donor is 1.62 eV. All these effects imply that nitrogen and vanadium codoping is very beneficial for the separation of photoexcited electron–hole pairs, and thus can greatly enhance the photocatalytic activity of TiO_2.

On the basis of the electronic band structure, the optical absorption spectra of pure polycrystalline anatase TiO_2 between 300 and 800 nm were calculated. The results are shown in Fig. 4. For these calculations, the scissors operator applied was 0.58 eV, accounting for the difference between the experimental band gap (3.23 eV) and the calculated band gap (2.55 eV). This curve for pure anatase

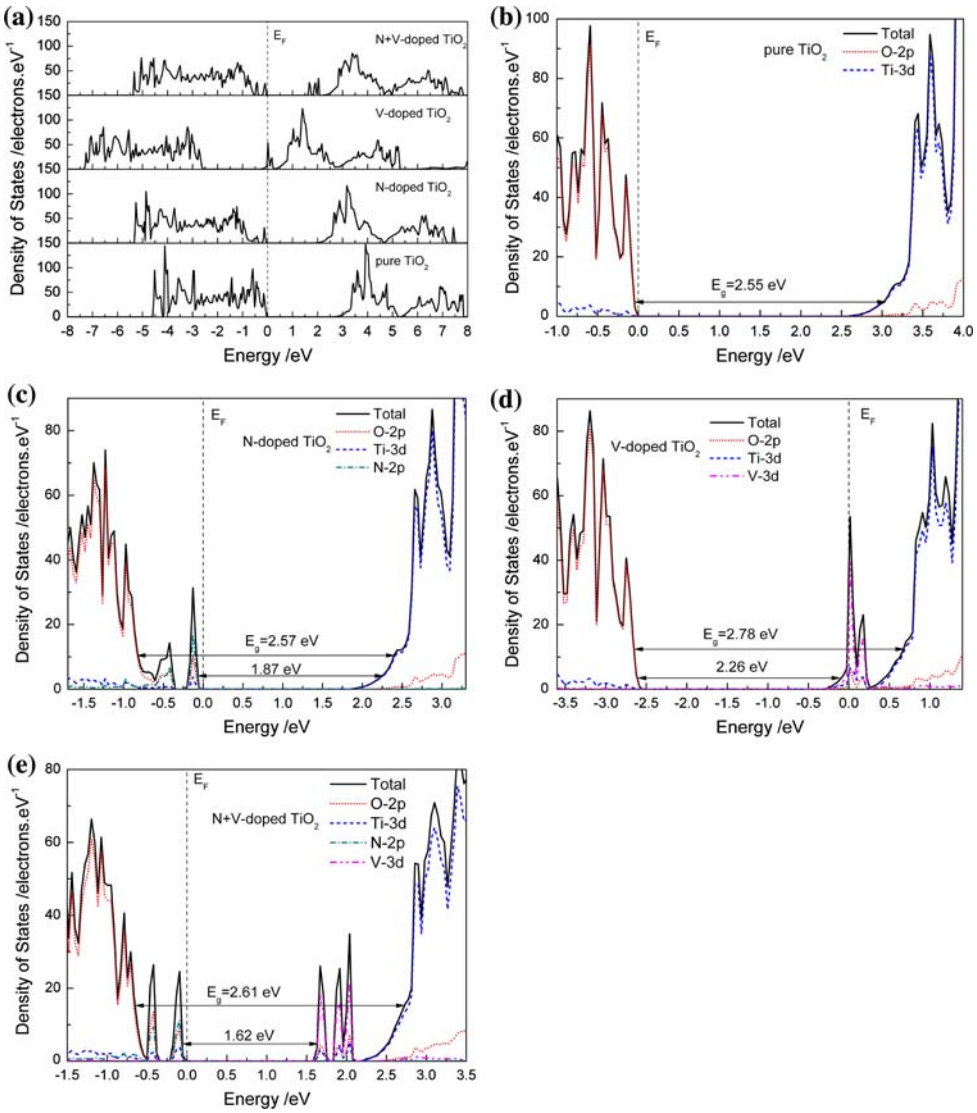

Fig. 3 (**a**) Calculated and comparison TDOS of different ions doped TiO_2; Calculated PDOS of (**b**) pure TiO_2, (**c**) N-doped TiO_2, (**d**) V-doped TiO_2, and (**e**) N + V-doped TiO_2 around the band gap

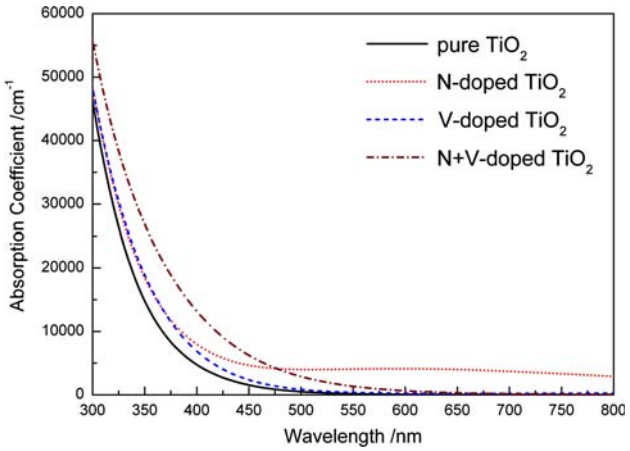

Fig. 4 The optical absorption curves of calculated for various types ion-doped TiO_2

TiO_2 accords with experiment very well [33], and will be used as a benchmark for comparing the results from N-doped, V-doped and N + V-doped TiO_2 calculations. We found that the fundamental absorption edges red-shift toward visible-light region by nitrogen or vanadium doping. This phenomenon is obvious for N + V-doped TiO_2 than that of N-doped or V-doped TiO_2. So the optical absorbance curves for the N + V-doped TiO_2 shows the highest photoresponse for visible-light. In particularly, there is certain absorption coefficient for N-doped TiO_2 in visible-light region. But this part of light absorption might not very useful for enhancing photocatalysis of TiO_2 owing to relative lower electronic occupied rate as shown in Fig. 3c.

The ability of a semiconductor to undergo photoexcited electron transfer to adsorbed species on its surface is governed by the band energy position of the semiconductor and the redox potentials of the adsorbate. The relevant potential level of the acceptor is thermodynamically required to be below (more positive than) the conduction

band potential of the semiconductor. The potential level of the donor needs to be above (more negative than) the valence band position of the semiconductor in order to donate an electron to the vacant hole [34]. So, we also calculated the band edge position of the photocatalyst according to the electronegativity of the oxide. Here in the electronegativity of an atom is the arithmetic mean of the atomic electron affinity and the first ionization energy, other than the common-defined term. The CB edge position of a semiconductor at the point of zero charge can be expressed empirically by [35, 36]:

$$E_{CB} = X - E^{e} - 0.5E_{g} \quad (2)$$

where E_{CB} is the CB edge potential, X is the electronegativity of the semiconductor which is the geometric mean of the electronegativity of the constituent atoms. E^{e} is the energy of free electrons on the hydrogen scale ($\sim$4.5 eV), and E_{g} is the band gap energy of the semiconductor. According to this expression, the rough CB edge potential of TiO_2 is -0.303 eV with respect to the normal hydrogen electrode. Subsequently the edge position of the VB of the photocatalyst is determined as 2.927 eV based on its band gap energy. This result is very consistent with the band energy position of TiO_2 in Ref. [34]. In Fig. 5, we plotted the band energy position of different ions doped TiO_2. It is well known that H_2O_2 and O_3 can oxide many organics because they have strong oxidative potential 1.77 eV (H_2O_2) and 2.07 eV (O_3). Compared with them, N-doped, V-doped and N + V-doped TiO_2 photocatalysts have excellent redox ability. Moreover, comparing with that of pure TiO_2, the CB edges are slightly upper shifting, and the VB edges are slightly downward shifting. This means that nitrogen or vanadium doping could enhance the redox potentials of TiO_2.

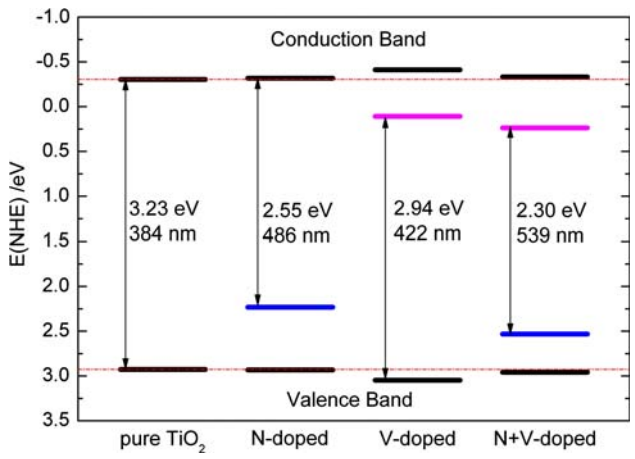

Fig. 5 The calculated band energy position of different ions doped TiO_2. The band gaps and corresponding wavelength threshold were corrected by "scissors operator" in this figure

4 Conclusion

In summary, by means of the first-principles calculation, we designed highly effective photocatalyst of anatase TiO_2 codoped with nitrogen and vanadium that can response for visible-light. The calculated results shown that nitrogen and vanadium codoping can effectively red-shifted the fundamental absorption edge of TiO_2. It simultaneously has shallow acceptor and shallow donor in the band gap, and has local internal fields, which enable photoexcited electron–hole pairs' separation become very easily. On the other hand, the band edge was slightly changed by cod-oping, so it has stronger redox potential than that of pure TiO_2. All the effects result in a significant improvement for the photocatalytic activity of TiO_2 under visible-light irradiation. Thus, nitrogen and vanadium codoping TiO_2 photocatalyst that we designed in this article is meeting the requirement of highly effective photocatalyst.

Acknowledgments This work was financially supported by the Program for the New Century Excellent Talents in University of Ministry of Education, China (Grant No. NCET-04-0915), the Natural Science Foundation of Yunnan province, China (Grant No. 2005E0007M). The authors thank High Performance Computer Center of Yunnan University for providing software and hardware support in our calculations.

References

1. Fujishima A, Honda K (1972) Nature 238:37
2. Tang J, Zou Z, Ye J (2004) Catal Lett 92:53
3. Volodin AM (2000) Catal Today 58:103
4. Gole JL, Stout JD, Burda C, Lou Y, Chen X (2004) J Phys Chem B 108:1230
5. Anpo M, Takeuchi M (2003) J Catal 216:505
6. Asahi R, Morikawa T, Ohwaki T, Aoki K, Taga Y (2001) Science 293:269
7. Ohno T, Akiyoshi M, Umebayashi T, Asai K, Mitsui T, Matsumura M (2004) Appl Catal A 98:255
8. Anpo M, Takeuchi M (2003) J Catal 216:505
9. Fujii H, Inata K, Ohtaki M, Eguchi K, Arai H (2001) J Mater Sci 36:527
10. Otaka H, Kira M, Yano K, Ito S, Mitekura H, Kawata T, Matsui F (2004) J Photochem Photobiol A: Chem 164:67
11. Dengwei J, Yaojun Z, Liejin G (2005) Chem Phys Lett 415:73
12. Zhao W, Ma WH, Chen CC, Zhao JC, Shuai ZG (2004) J Am Chem Soc 126:4782
13. Luo HM, Takata T, Lee Y (2004) Chem Mater 16:846
14. Liu HY, Gao L (2004) Chem Lett 33:730
15. Segall MD, Lindan PJD, Probert MJ, Pickard CJ, Hasnip PJ, Clark SJ, Payne MC (2002) J Phys: Condens Matter 14:2717
16. Ceperley DM, Alder BJ (1980) Phys Rev Lett 45:566
17. Perdew JP, Zunger A (1981) Phy Rev B 23:5048
18. Godby RW, Schluter M, Sham LJ (1988) Phys Rev B 3:10159
19. Burdett JK, Hughbandks T, Miller GJ, Richardson JW, Smith JV (1987) J Am Chem Soc 10:3639
20. Cui XY, Medvedeva JE, Delley B, Freeman AJ, Newman N, Stampfl C (2005) Phys Rev Lett 95:256404
21. Hong NH, Sakai J, Hassini A (2004) Appl Phys Lett 84:2602

22. Du XS, Li QX, Su H, Yang J (2006) Phys Rev B 74:233201
23. Sato J, Kobayashi H, Inoue Y (2003) J Phys Chem B 107:7970
24. Li H, Zhao G, Han G, Song B (2007) Surf Coat Tech 201:7615
25. Shen H, Mi L, Xu P, Shen W, Wang PN (2007) Appl Surf Sci 253:7024
26. Lee JY, J Park, Cho JH (2005) Appl Phys Lett 87:011904
27. Long MC, Cai WM, Wang ZP, Liu GZ (2006) Chem Phys Lett 420:71
28. Goodenough JB, Hamnett A (1984) In: O. Madelung (ed) Landolt-Börnsterin, new series, vol III/17 g. Springer Verlag, Berlin, p. 133
29. Stampfl C, Van de Walle CG (1999) Phys Rev B 59:5521
30. Perdew JP, Levy M (1983) Phys Rev Lett 51:1884
31. Asahi R, Taga Y, Mannstadt W, Freeman AJ (2000) Phys Rev B 61:7459
32. Tang J, Ye J (2005) Chem Phys Lett 410:104
33. Boschloo GK, Goossens A, Schoonman J (1997) J Electronchem Soc 144:1311
34. Amy LL, Guangquan L, Yates JT Jr (1995) Chem Rev 95:735
35. Nethercot AH (1974) Phys Rev Lett 33:1088
36. Junwan T, Jinhua Y (2005) Chem Phys Lett 410:104